

This article was downloaded by:

On: 24 January 2011

Access details: *Access Details: Free Access*

Publisher *Taylor & Francis*

Informa Ltd Registered in England and Wales Registered Number: 1072954 Registered office: Mortimer House, 37-41 Mortimer Street, London W1T 3JH, UK



Journal of Macromolecular Science, Part A

Publication details, including instructions for authors and subscription information:

<http://www.informaworld.com/smpp/title~content=t713597274>

Study of Thermo- and Photooxidation of Head-To-Tail and Head-to-Head Polystyrene Films

M. Iring^a; M. Szesztay^a; A. Stirling^a; F. Tüdös^{ab}

^a Central Research Institute for Chemistry Hungarian Academy of Sciences, Budapest, Hungary ^b

Department of Chemical Technology Eötvös, Lorand University 1117 Budapest, sétány 2, Hungary

To cite this Article Iring, M. , Szesztay, M. , Stirling, A. and Tüdös, F.(1992) 'Study of Thermo- and Photooxidation of Head-To-Tail and Head-to-Head Polystyrene Films', *Journal of Macromolecular Science, Part A*, 29: 10, 865 – 884

To link to this Article: DOI: 10.1080/10601329208054124

URL: <http://dx.doi.org/10.1080/10601329208054124>

PLEASE SCROLL DOWN FOR ARTICLE

Full terms and conditions of use: <http://www.informaworld.com/terms-and-conditions-of-access.pdf>

This article may be used for research, teaching and private study purposes. Any substantial or systematic reproduction, re-distribution, re-selling, loan or sub-licensing, systematic supply or distribution in any form to anyone is expressly forbidden.

The publisher does not give any warranty express or implied or make any representation that the contents will be complete or accurate or up to date. The accuracy of any instructions, formulae and drug doses should be independently verified with primary sources. The publisher shall not be liable for any loss, actions, claims, proceedings, demand or costs or damages whatsoever or howsoever caused arising directly or indirectly in connection with or arising out of the use of this material.

STUDY OF THERMO- AND PHOTOOXIDATION OF HEAD-TO-TAIL AND HEAD-TO-HEAD POLYSTYRENE FILMS†

M. IRING, M. SZESZTAY, and A. STIRLING

Central Research Institute for Chemistry
Hungarian Academy of Sciences
H-1525 Budapest, POB 17, Hungary

F. TÜDÖS*

Central Research Institute for Chemistry
Hungarian Academy of Sciences
H-1525 Budapest, POB 17, Hungary

Department of Chemical Technology
Eötvös Loránd University
1117 Budapest, Pázmány P. sétány 2, Hungary

ABSTRACT

A study was made on the thermo- and photooxidation of head-to-tail (PS) and head-to-head (H-HPS) polystyrene films. The process was followed by determination of the overall oxygen uptake (conversion), IR spectrum, molecular mass distribution, and carboxyl group concentration. The mechanism of the process depends on the type of initiation (thermal or photo). For either the thermally initiated or photoinitiated process, the mechanism depends very little on the structure of the poly-

†This paper is based on cooperative work with Professor Otto Vogl on the comparative autoxidation of head-to-head and head-to-tail polyolefins and poly(vinyl halides). It is dedicated to Otto Vogl on the occasion of his 65th birthday.

mer, but the oxidation of H-HPS is much faster. This can be ascribed to the higher concentration of structural defects (mainly double bonds) in H-HPS and not to the difference in the basic structure of the polymers. In thermal oxidation, at least three carbonyl groups with different structures, phenolic hydroxyl groups, and a small quantity of carboxyl groups could be detected. Plotting the carbonyl concentration against conversion resulted in a more or less linear function. The concentration of phenolic hydroxyl groups was found to increase slightly with oxygen pressure (p). Thus, the rate of oxidation slightly decreases with increasing p (more pronounced autoinhibition). The fragmentation taking place in thermal oxidation and the carbonyl formation are connected. Hydroperoxide, carboxyl, and (mainly ester) carbonyl groups can be detected in photooxidation. Head-to-tail PS is fragmented very slightly in this process, while oxidized dimers and trimers are eliminated from H-HPS.

INTRODUCTION

The photooxidation of commercial polystyrene (PS) is the source of many technical problems. For that reason the process has been investigated in the last 40 years by many authors, both from scientific and practical points of view [1].

It is known that chemically pure PS does not absorb in the energy range of sunlight, so the investigations have been aimed partly at the elucidation of the structure [2, 5] and formation [6] of chromophores initiating the process and partly at filling out the mechanism and kinetics of the entire photooxidation sequence [1, 7-9].

The thermally initiated oxidation of PS is a less studied process [10-13], notwithstanding that it proceeds at the temperature of processing and results in the formation of chromophores which promote later photooxidation of the polymer [6]. The results on thermal oxidation are sometimes controversial [10, 13, 14].

Information relating to the similarities and/or differences in the mechanisms of the photo- and thermooxidation is also limited, and results have frequently been obtained from experiments made in a solvent or on model compounds [10, 15, 16].

Beside the common head-to-tail polystyrene structure formed in the industrial polymerization process, there also exists PS with a head-head structure (H-HPS) as synthesized by Vogl and coworkers [17]. Its behavior in thermo- and photooxidation is scarcely known [18].

In the present work we report on and compare the kinetics of oxygen uptake and the formation of oxidation products as well as on the change in molecular mass in the thermo- and photooxidation of both head-to-tail PS and H-HPS.

EXPERIMENTAL

Polymers

Purified commercial Kristen 144 and H-HPS synthesized by the method of Ref. 17 and characterized in Ref. 14 were used in the present experiments.

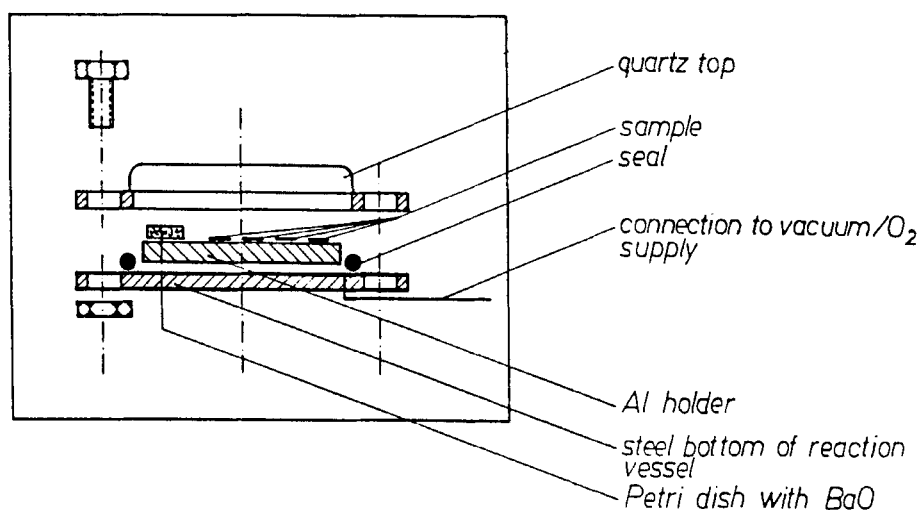


FIG. 1. Scheme of the sample holder used in the photooxidation.

Oxidation Technique and Conditions

Thermal Oxidation

Thermal oxidation was carried out in equipment suitable for following the kinetics of oxygen absorption [19].

Photooxidation

To follow oxygen uptake during photooxidation, we designed a special reaction vessel and connected it to the same equipment used for thermal oxidation measurements.

The scheme of the sample holder can be seen in Fig. 1. Four layers of the polymer film were placed on an aluminum holder together with a Petri dish containing BaO (BaO absorbs H₂O and CO₂ evolved during oxidation). The holder with the samples was put in a reaction vessel equipped with a top made of quartz. The reaction vessel and a reference vessel were immersed in a water bath at 30°C. A HgO 250 source was used to irradiate the sample. The distance between the vessels and the irradiation source was 330 mm.

The oxidation conditions are summarized in Table 1.

TABLE 1. Conditions of Oxidation

	Thermal oxidation	Photooxidation
Temperature, °C	160-190	30
O ₂ pressure, kPa	6-101	101
Film thickness, μm	20-150	50

Methods

Methods applied for the characterization of untreated and oxidized samples are summarized in Table 2.

To evaluate the rate of formation of carbonyl and hydroxyl groups, the mid-infrared spectra of polymers were recorded with a BOMEM MB 102 FTIR system. The thermooxidized polymers were studied as films on a KBr pellet, while the photooxidized polymers were self-supporting films.

The evaluation of spectra was done as follows: The spectrum of the original polymer was subtracted from the spectrum of the oxidized polymer in order to obtain a differential spectrum. The integrated intensity of the chosen peak in the differential spectrum was divided by the integrated intensity of a reference peak (depending only on the concentration of the polymer and not on the degree of oxidation) from the original spectrum of the polymer; $\nu = 1944 \text{ cm}^{-1}$ was chosen as suitable.

The bands chosen from the spectra of the photooxidized polymers and from the spectra of the thermooxidized polymers to characterize the oxidation process can be seen in Figs. 2 and 3, respectively.

GPC measurements were made on a Waters ALC-GPC-201 instrument equipped with two detectors: RI 400 and UV-440 with a filter for 254 nm [14].

RESULTS

Kinetics of Oxygen Uptake

The kinetics of oxygen uptake were investigated for PS over a broad range of pressures and film thicknesses at 190°C. Figure 4 shows the oxygen uptake curves recorded at different pressures. As can be seen, the induction period of oxygen uptake is higher at 6.6 kPa than at higher pressures. Above ~10 kPa, however, the initial stages of the curves do not differ substantially from one another. Further experiments were carried out at 101 kPa.

Figure 5 shows the kinetic curves of oxygen uptake of samples with various thicknesses.

The initial rate of oxidation decreases with increasing sample thickness above ~50 μm ; that is, the thermal oxidation becomes diffusion controlled. Our further experiments were therefore carried out on films of 50 μm thickness.

TABLE 2. Methods of Investigation

Property	Method/Reference
Kinetics of oxygen uptake	Gas-volumetric [19]
Concentration of carboxylic groups	Acidi-alkalimetry [20]
Concentration of carbonyl and hydroxyl groups	IR analysis
Molecular mass change	GPC [21]

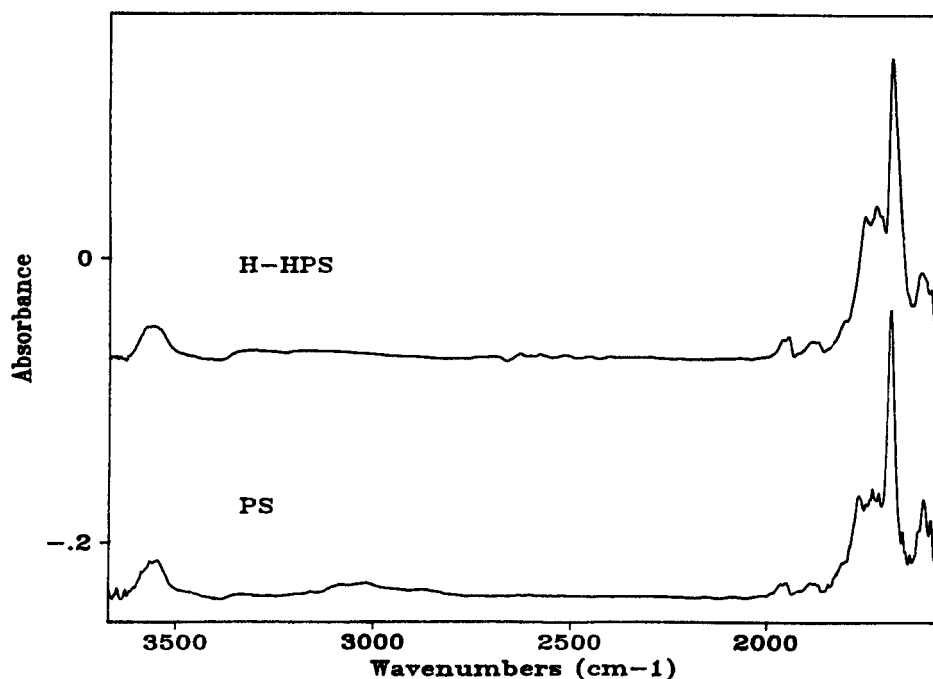


FIG. 2. IR bands chosen to characterize the oxidized structures in the thermooxidation of PS and H-HPS.

Figure 6 illustrates the kinetic curves of oxygen uptake for PS and H-HPS recorded at various temperature [oxygen pressure (p), 101 kPa; sample thickness, 50 μm]. The curves are of similar character, but the rate of oxygen uptake is higher for H-HPS. The kinetic curves reflect the results of several processes (radical oxidation, inhibited oxidation, and possibly the formation of volatile organic substances). At the points marked by arrows, the reaction vessel was evacuated and refilled with oxygen. The exchange of atmosphere caused a marked increase of the rate, especially for H-HPS.

The time dependence of oxygen uptake in the photooxidation of PS and H-HPS is illustrated in Fig. 7. The reaction rate is decelerating for both polymers. The rate of photooxidation of H-HPS considerably exceeds that of PS, and it temporarily increases when the atmosphere is exchanged.

Formation of Oxygen-Containing Groups

The change in concentration of $>\text{CO}$ and $-\text{OH}$ groups was followed by the intensity change of the assigned bands of the IR spectrum (see Figs. 2 and 3). The spectra also refer to the difference in mechanisms of thermo- and photooxidation.

In the spectra of the thermooxidized polymers we have a broad band in the 1650–1845 cm^{-1} region. This band is a superposition of at least three different peaks. One of them is at 1685 cm^{-1} , and the others are at 1730 and ~ 1770 cm^{-1} .

The spectra of the photooxidized polymers in the carbonyl region are much less complex. There is a strong peak at 1730 cm^{-1} (see Fig. 3).

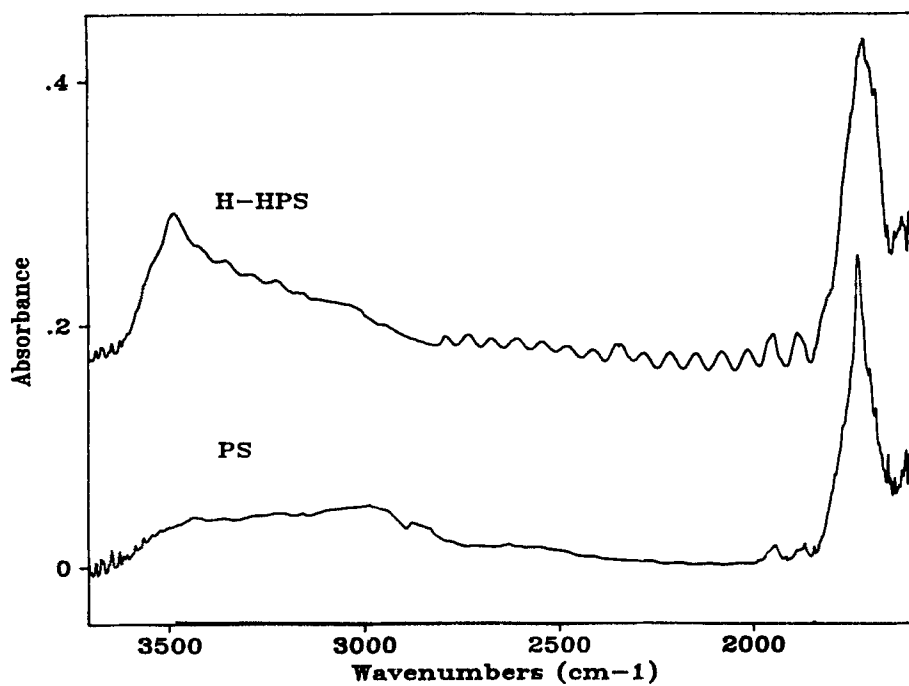


FIG. 3. IR bonds characterizing the oxidized structures in the photooxidation of PS and H-HPS.

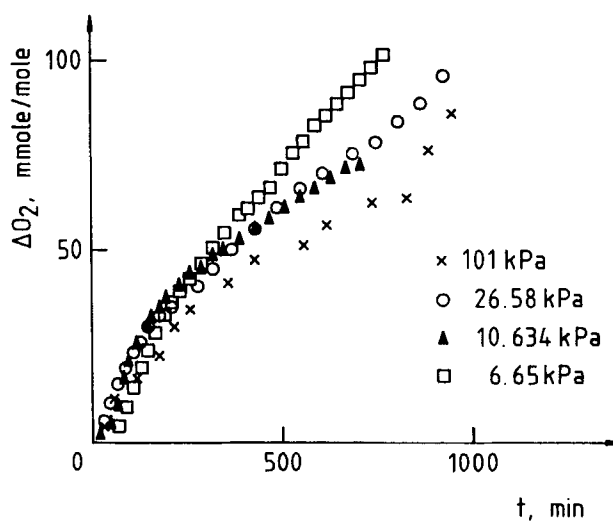


FIG. 4. Time dependence of oxygen uptake in thermal oxidation of PS at different oxygen pressures (190°C, 50 μm thickness).

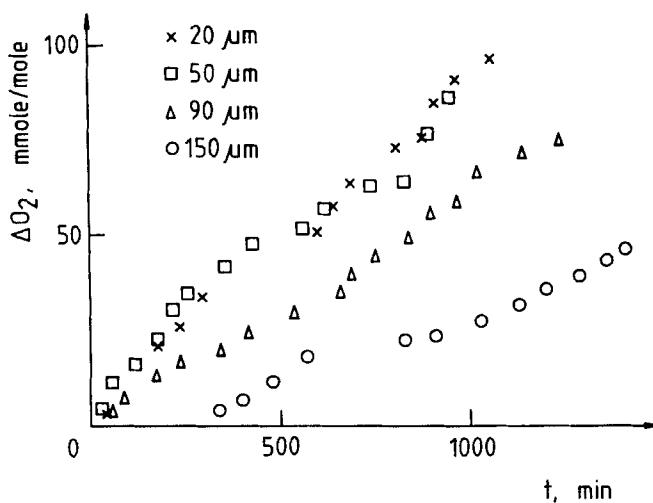


FIG. 5. Time dependence of oxygen uptake in the thermal oxidation of PS at different film thicknesses (190°C, 101 kPa).

A well-defined band can be seen in the $-\text{OH}$ region at 3545 cm^{-1} in the thermooxidized PS and at 3568 cm^{-1} in H-HPS. These bands most probably belong to phenolic OH.

In the $2780\text{--}3650\text{ cm}^{-1}$ region there is a very broad band due to some different $-\text{OH}$ group in the photooxidized samples. A part of this band ($2780\text{--}3100$) belongs to the uncompensated $\text{C}-\text{H}$ stretching vibrations.

The integrated relative intensities of these peaks (related to the intensity of the peak at 1944 cm^{-1}) were determined, and their dependence on the oxygen uptake was examined.

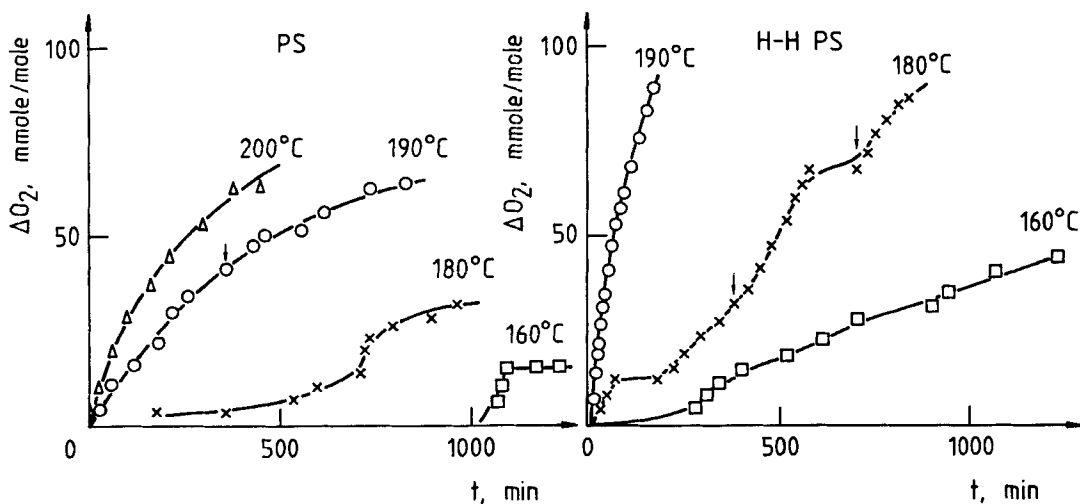


FIG. 6. Time dependence of oxygen uptake in the thermal oxidation of PS and H-HPS at different temperatures (101 kPa, $50\text{ }\mu\text{m}$).

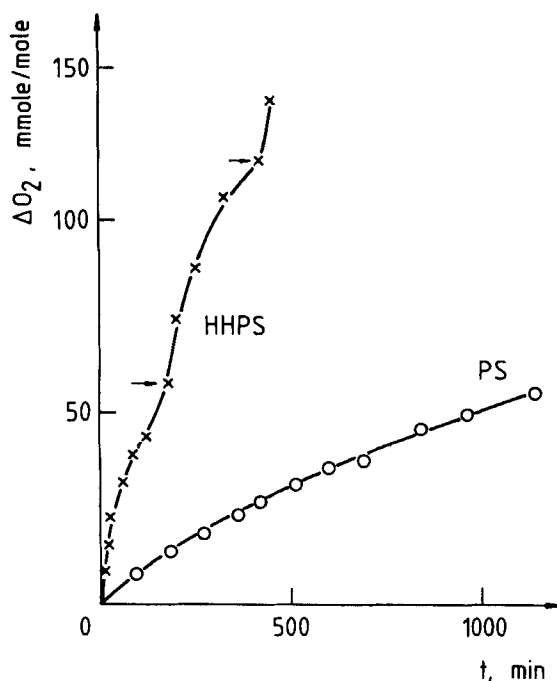


FIG. 7. Time dependence of oxygen uptake in the photooxidation of PS and H-HPS (30°C, 101 kPa, 50 μ m).

Figure 8 shows the integral absorption values characteristic of carbonyl groups and related to the polymer concentration $\{A(\Sigma\text{CO})/A(\nu=1944) = A(\text{CO}),\text{rel}\}$ plotted against oxygen uptake in the thermal oxidation of PS under different oxidation conditions. The scattering of the data is high, owing to the nature of the system investigated. It is clear, however, that the amount of carbonyl groups increases with ΔO_2 , independent of the oxidation conditions. An analogous relationship was obtained earlier for H-HPS [14].

The relative integral absorptions of the polymers measured in the hydroxyl region $\{A(\Sigma\text{OH})/A(\nu=1944) = A(\text{OH}),\text{rel}\}$ against the oxygen uptake at different oxygen pressures are illustrated in Fig. 9. The rate of formation of —OH groups depends on the oxygen pressure. At low pressure (6.65 kPa), slight —OH formation takes place at the initial stage of the process, while at 101 kPa the highest rate occurs at time $t = 0$. The value of the $A(\text{OH}),\text{rel}$ related to the same conversion is significantly lower at lower pressure.

Although the data scatter is rather high, we decided that the relationship is not linear. On the high pressure curve we also indicate a value belonging to H-HPS. As can be seen, these data are not separate from the values for head-to-tail PS.

The dependence of the relative integral absorption of the carbonyl group (measured in photooxidation) on oxygen uptake is shown in Fig. 10 for both polymers. The curve is nonlinear, has the character of a saturation curve, and does not show any significant dependence on polymer structure.

Figure 11 illustrates the $A(\text{OH})_{\text{rel}}$ data as a function of ΔO_2 . In disagreement with the above observations, $A(\text{OH})_{\text{rel}}$ vs ΔO_2 cannot be plotted on the same curve for both polymers. The concentration of $-\text{OH}$ groups is higher in PS than in H-HPS at the same conversion.

Carboxyl groups also form in the thermo- and photooxidation of head-to-tail PS and HH-PS, but in higher amount in H-HPS. The data shown in Fig. 12 have extensive scatter (those for head-to-tail PS show even more scatter).

A higher quantity of carboxyl groups forms in photooxidation (see Fig. 13), and this amount seems to increase proportionally with oxygen uptake.

The data scatter was very high in the studies of both processes. Therefore, the idea arose that the carboxyl groups formed might decompose during the "storage time" between oxidation and analysis or, by being bound to volatile small molecules, they might escape from the film. That is why the change in the value of $[-\text{COOH}]$ was investigated against storage time after oxidation of head-to-tail PS. The results are shown in Fig. 14.

A decrease of about 27% in $[-\text{COOH}]$ was found in the first week. Later, the change was much slower. The scattering observed can only partly be explained by this factor; the other causes are not known.

Molecular Mass Distribution (MMD)

It was reported that both scission and coupling processes take place during the oxidation of PS [1, 13]. Therefore, the molecular mass distribution of the

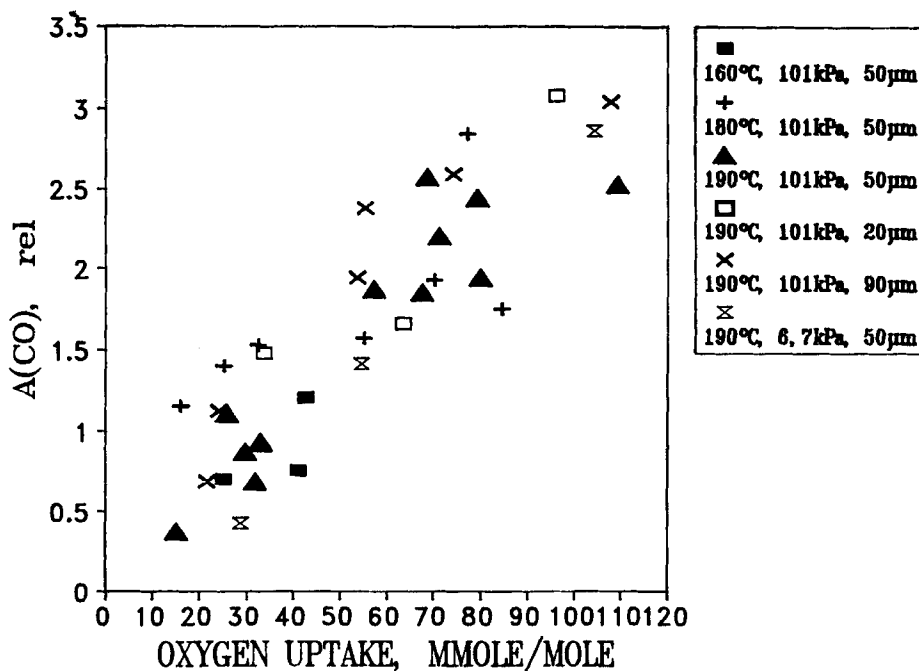


FIG. 8. Change in the values of $A(\text{OH})_{\text{rel}}$ as a function of the overall oxygen uptake in the thermooxidation of PS at different conditions of oxidation.

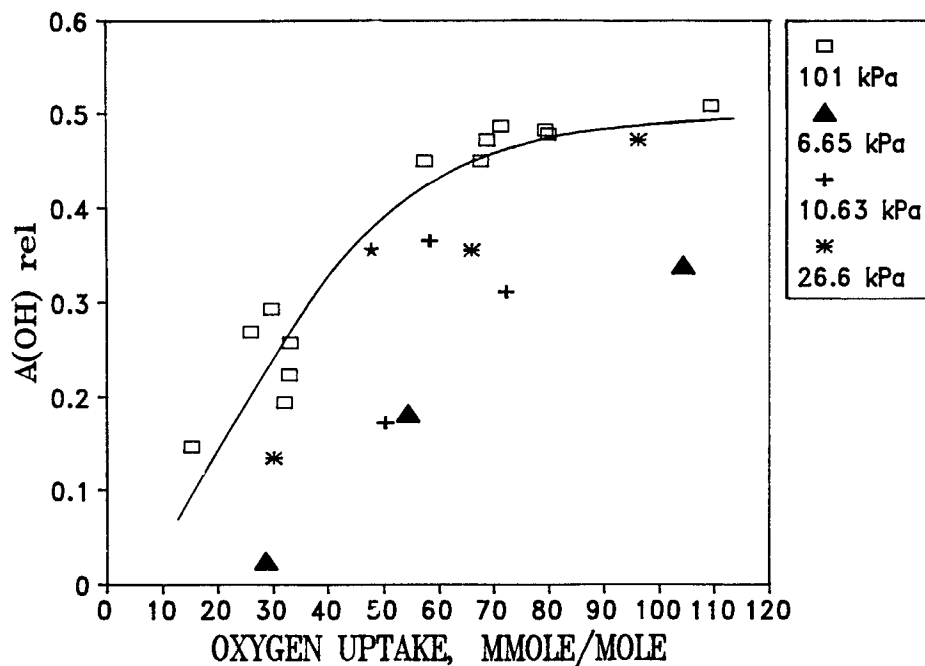


FIG. 9. Change in the values of $A(\text{OH})_{\text{rel}}$ as a function of the overall oxygen uptake at different oxygen pressures in the thermooxidation of PS (190°C, 50 μm). (The asterisks indicate data for H-HPS.)

soluble fraction of oxidized polymer was studied by the GPC method by using an RI detector. From the number-average molecular mass values calculated from the distribution curves, the average fragmentation number, $s = (\overline{M}_{n,0}/\overline{M}_{n,t}) - 1$, was determined.

In thermooxidation, the amount of soluble molecule fragments increases proportionally to the oxygen uptake for both polymers, as shown by the data for head-to-tail PS in Fig. 15. The fragmentation number at the same oxygen uptake was found to be somewhat lower in H-HPS. This may be related to the more intensive gel formation in H-HPS and not to its higher stability.

We emphasize again that UV detection is not suitable for following the fragmentation process taking place in oxidized PS and H-HPS. A distorted curve is obtained by the UV detector. The extinction is not proportional to the concentration. At the same time, the shapes of the curves give some information about more complex characteristics of the mechanism of oxidation (see Figs. 19 and 20).

In Fig. 16 the value of s is plotted against ΔO_2 for the photooxidation of both polymers. As can be seen, PS is not fragmented much in photooxidation, or else simultaneous coupling of molecules connected with gel formation and crosslinking takes place, while in the case of H-HPS a considerably greater extent of fragmentation occurs.

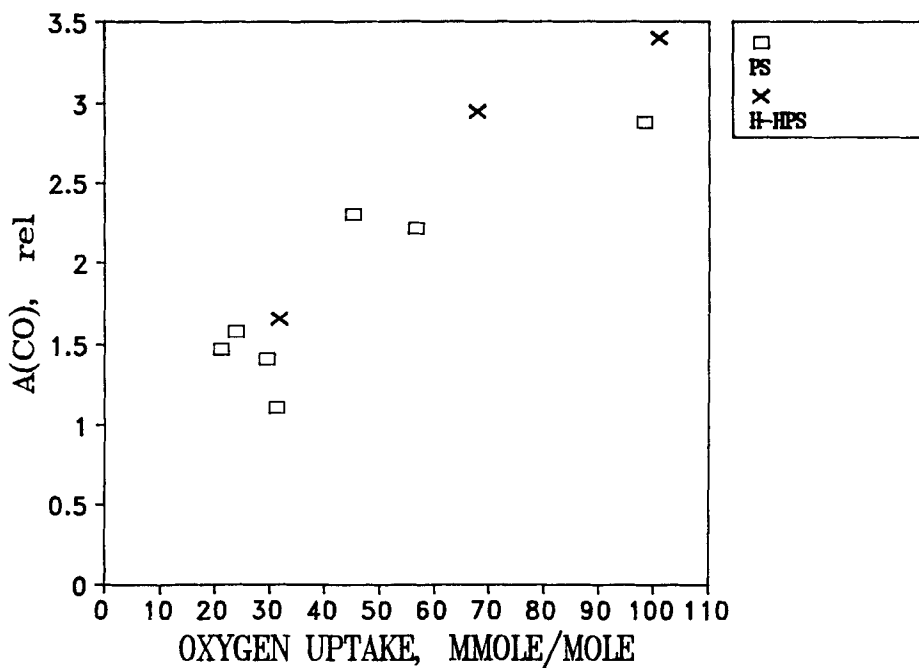


FIG. 10. $A(\text{CO}), \text{rel}$ vs ΔO_2 in the photooxidation of head-to-tail PS and H-HPS.

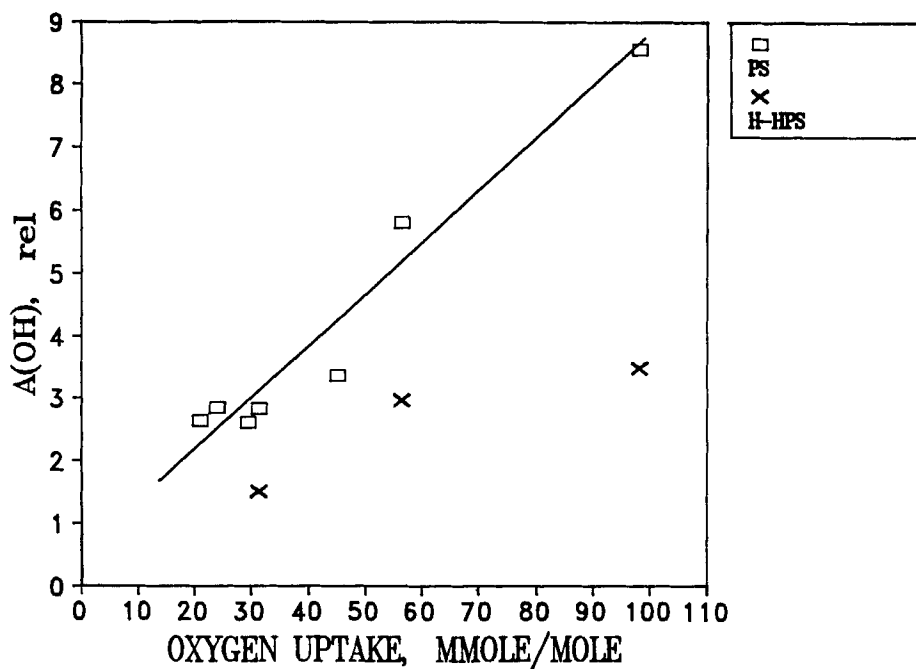


FIG. 11. $A(\text{OH}), \text{rel}$ vs ΔO_2 in the photooxidation of head-to-tail PS and H-HPS.

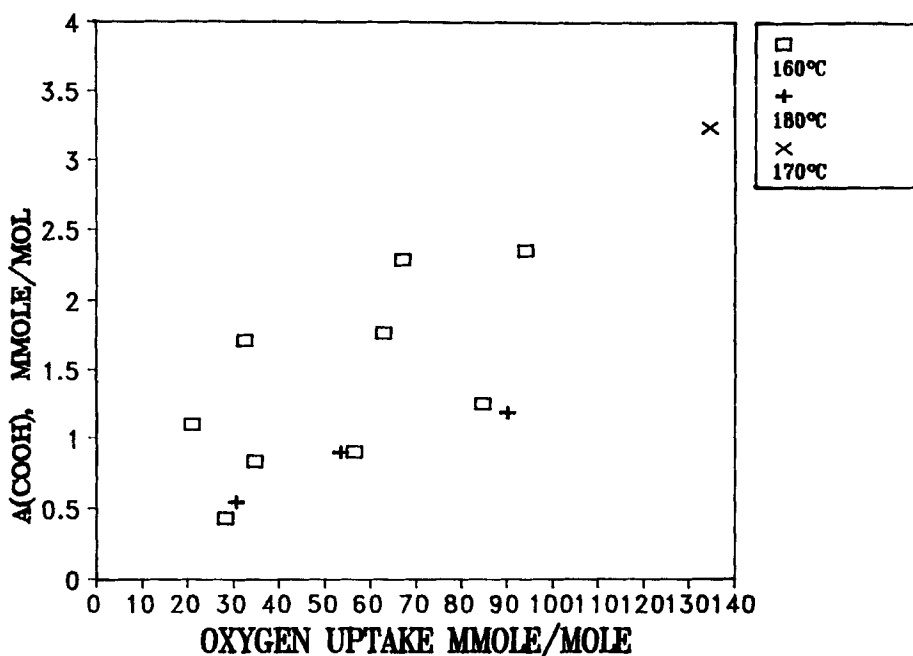


FIG. 12. Concentration of carboxyl groups as a function of overall oxygen uptake in the thermal oxidation of H-HPS.

DISCUSSION

Figures 6 and 7 suggest that there is no marked difference between the oxygen uptake kinetics of PS and H-HPS. The rate of oxidation of H-HPS is, however, higher at the same temperature. This can be ascribed to the higher concentration of structural defects—mainly double bonds (see Table 1 in Ref. 14)—in H-HPS and not to the difference in the basic structures of the polymers. In thermal oxidation, the shape of the curves depends on the temperature. At high temperature ($T = 190^{\circ}\text{C}$) relatively simple decelerating kinetics can be observed, while more complex curves are obtained at lower temperatures ($160\text{--}180^{\circ}\text{C}$).

It is known that thermal oxidation of PS is a self-inhibiting process [11]. If the inhibitor concentration exceeds a certain value, the process will slow down. When the inhibitor concentration is decreased, the process accelerates again. At higher temperatures the inhibition effect generally becomes weaker [22].

The complexity of the mechanism of thermal oxidation is indicated by the complexity of the composition of products observed in the IR spectra of both polymers. In the absorption region of carbonyl groups, at least three maxima can be seen (see Fig. 2): at 1684 , 1730 , and 1770 cm^{-1} . A similar spectrum is given by Rånby et al. for photooxidized PS. The band observed at 1684 cm^{-1} is assigned to the acetophenone structure [9], but there is no uniform assignment for the bands at 1730 and 1770 cm^{-1} .

The absorption at 1730 cm^{-1} is generally assigned to an aliphatic aldehyde group, while the keto-lactone ring absorbs at 1770 cm^{-1} as claimed by Ref. 15.

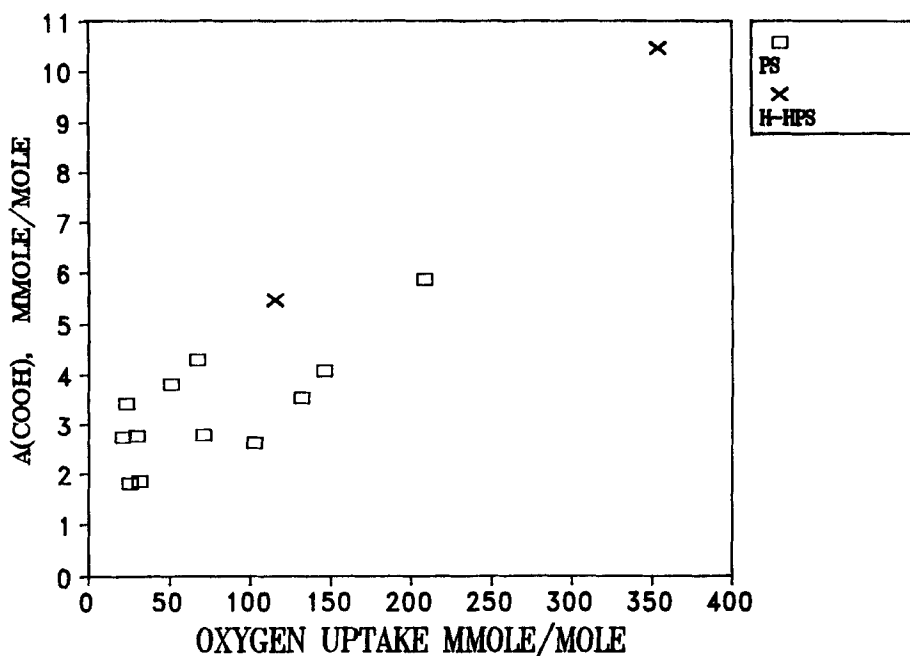


FIG. 13. Concentration of carboxyl groups as a function of overall oxygen uptake in the photooxidation of head-to-tail PS and H-HPS.

In photooxidation the absorption band characteristic to the >CO group is similar for both polymers, and it is much less complex (see Fig. 3) than in thermal oxidation. A strong band dominates, with an absorption maximum at 1730 cm^{-1} . Another broad band can be observed in the spectrum at about 1240 cm^{-1} . These bands probably belong to an ester group (C=O and C-O-C stretching vibrations, respectively). This belief is supported by the fact that the ratio of the integrated intensity of these two peaks does not depend on the accumulated oxygen uptake.

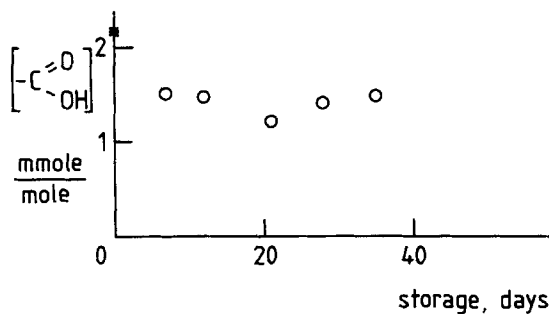


FIG. 14. Concentration of carboxyl groups formed in the thermal oxidation of head-to-tail PS as a function of the time passed between oxidation and analysis.

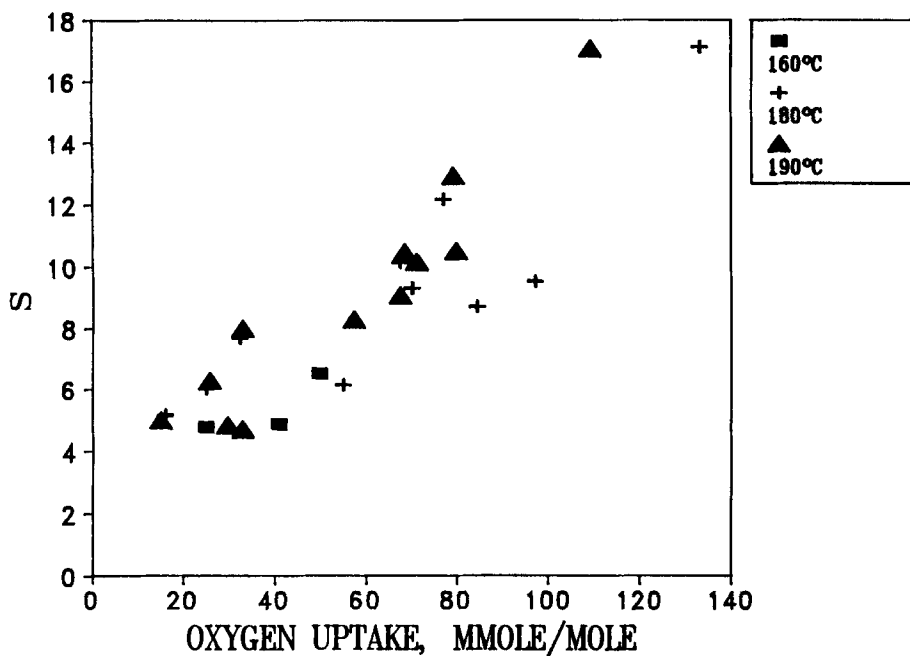


FIG. 15. Average number of scissions (s) as a function of overall oxygen uptake in the thermal oxidation of PS at different oxidation temperatures.

The absorption peaks obtained in the $-\text{OH}$ region are similar for each polymer in both their shape and wavelength range, and they depend on the mechanism of initiation (photo or thermal) only.

In thermal oxidation a well-defined, thermally stable band is observed in the $-\text{OH}$ range [14], and it can likely be assigned to a monosubstituted phenolic $-\text{OH}$ group. This seems to be supported by the observation that if an unoxidized PS film is kept in *o*-cresol vapor, the shape and maximum of the absorption peaks measured in the $-\text{OH}$ region are identical to those observed in thermooxidation, as can be seen in Fig. 17.

It is observed (see Fig. 9) that the absorption measured in the $-\text{OH}$ region at the same conversion is higher for H-HPS than for head-to-tail PS; that is, the proportion of phenolic $-\text{OH}$ groups formed is somewhat higher. In harmony with this, after the reaction vessel is evacuated and refilled with oxygen, the increase of the oxidation rate is higher with H-HPS than with head-to-tail PS. It can also be seen (Fig. 9) that the amount of $-\text{OH}$ groups formed at the same conversion depends on oxygen pressure. On the other hand, the ΔO_2 vs t plots (Fig. 4) indicate that, while the induction period for oxidation is longer and its initial rate is smaller at low pressure than at high pressure, this dependence is reversed and the rate of oxidation at lower pressures increases with increasing accumulated oxygen uptake. These two results suggest that the rate of formation of phenolic $-\text{OH}$ groups (which act as inhibitors of oxidation) depends on the oxygen pressure; the $-\text{OH}$ groups are probably the secondary products of the process.

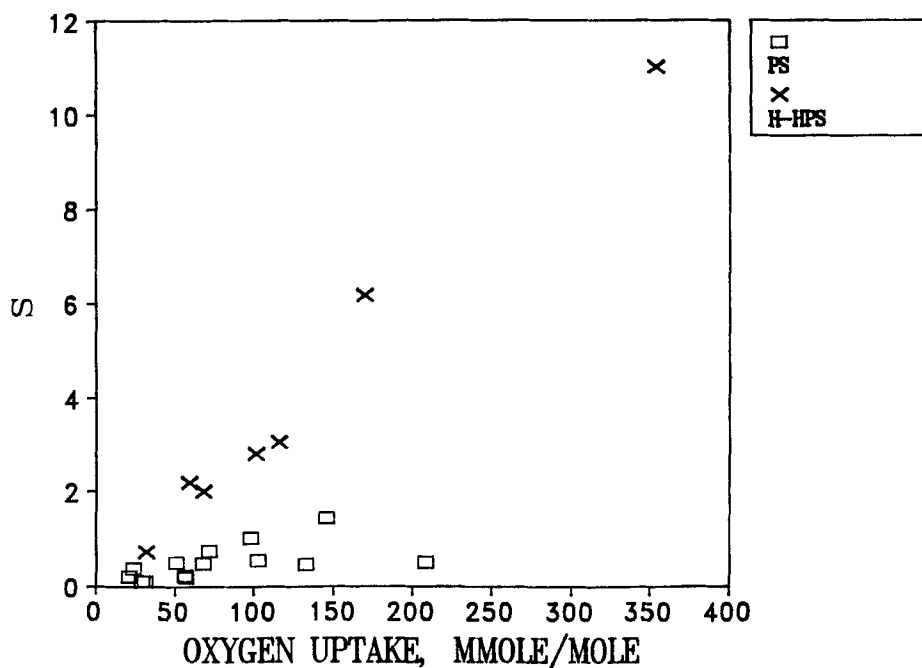


FIG. 16. Average number of scissions (s) as a function of overall oxygen uptake in the photooxidation of head-to-tail PS and H-HPS.

In the 2780–3650 cm^{-1} region there is a very broad band in the spectrum of each polymer (see Fig. 3) due to some different OH groups formed during photooxidation.

In contrast to the —OH structures formed in thermooxidation, part of those formed in photooxidation are thermally unstable. They decompose after 2 h at a heat treatment of 170°C as it can be seen in Fig. 18 for head-to-tail PS.

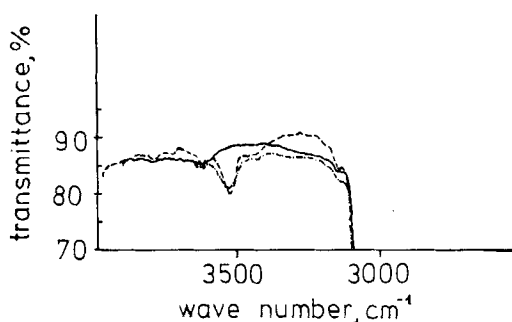


FIG. 17. Part of the IR spectra of thermally oxidized head-to-tail PS and that of unoxidized film treated in *o*-cresol vapor: unoxidized (—), oxidized (---), and treated in *o*-cresol vapor (-·-).

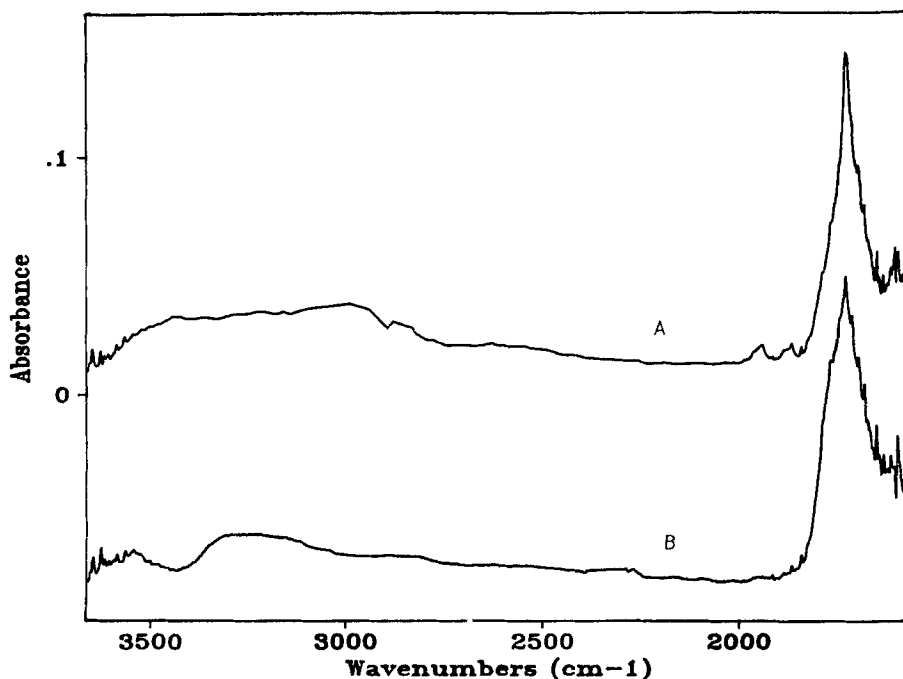


FIG. 18. IR spectra of photooxidized PS film before heating (a) and heated for 24 h at 170°C in vacuum (b) ($\Delta O_2 = 0.98$ mmol/g polymer).

It has been mentioned that the $W(\log M)$ vs $\log M$ plots representing fragmentation show a characteristic difference from the distribution curves representing UV activity. This fact was analyzed earlier with respect to the thermooxidation of head-to-tail PS and H-HPS [14]. While the mass distribution curves and the UV extinction traces in thermooxidation are similar for both polymers, significant differences have been found in photooxidation. In the latter (see Fig. 16), fragmentation of head-to-tail PS is minimal, but that of H-HPS is much greater.

Figures 19 and 20 show the mass distribution and UV extinction traces of head-to-tail PS and H-HPS samples oxidized to different conversions as a function of the molecular mass. Figure 19 indicates that in the case of head-to-tail PS, the distribution curves do not change much with increasing oxygen uptake, and their shape and range depend very little on the method of detection. In the case of H-HPS, as seen in Fig. 20, a small quantity (not detectable by RI) of molecular fragments with high UV activity is formed: they are mainly oxidized dimers and trimers. This experimental observation is probably connected with photoinitiation of the structural defects at the chain ends in H-HPS.

Further, the connections between quantities characteristic of the functional groups formed ($[-COOH]$, $A(CO)_{rel}$, $A(OH)_{rel}$) and the degree of fragmentation were investigated. It should be noted that the GPC measurement does not completely characterize the change in the molecular mass of the polymer. We have no special information about potential processes leading to gelation. The change in the average chain length of the polymer is denoted by s .

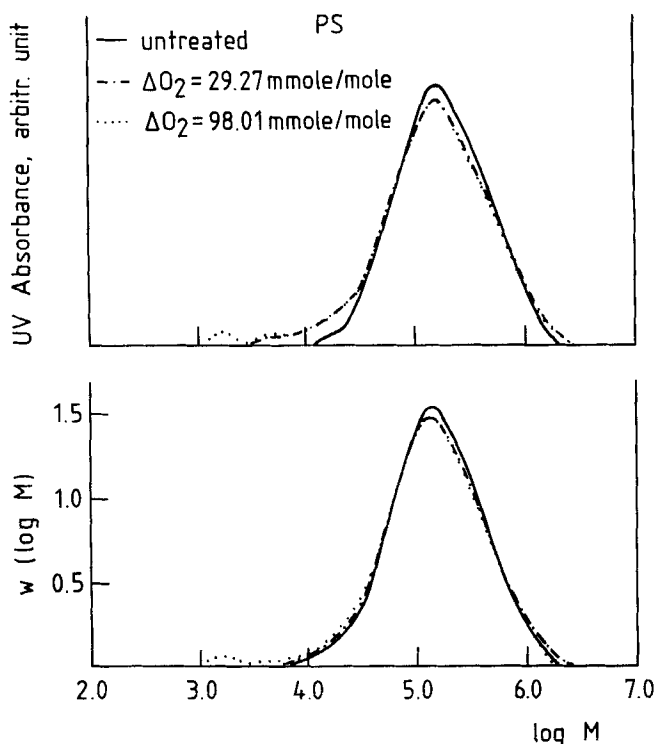


FIG. 19. Mass and UV distribution curves of untreated and photooxidized head-to-tail PS.

No definite relationship was found between the $[-\text{COOH}]$ values and the data obtained by UV detection in the thermal oxidation of head-to-tail PS and H-HPS. The formation of functional groups absorbing in the UV takes place independently of fragmentation processes, presumably by the formation of conjugated double bonds along the chain or of keto-lactone groups containing such bonds, as was described for the photooxidation of head-to-tail PS [15]. In spite of the great scatter, a certain correlation exists between the number of carboxyl groups and the s value characteristic of fragmentation, as can be seen in Fig. 21 for the case of H-HPS. We note that, at the same conversion, about half as many carboxyl groups were found in PS as in H-HPS. The $[-\text{COOH}]$ vs s relationship indicates that only a slight proportion of chain-scissions are accompanied by carboxyl group formation, in contrast to the observations with polyethylene [23].

The relation between IR absorption of $-\text{OH}$ groups and s value is shown in Fig. 22. In contrast to observations with carboxyl groups, the quantitative ratios were almost equal for both polymers, indicating at the same time that the value of $A(\text{OH})_{\text{rel}}$ is not considerably affected by the energy absorption of carboxylic $-\text{OH}$ groups.

The values of $A(\text{CO})_{\text{rel}}$ correlate with s very well, as illustrated in Fig. 23 for both polymers. The correlation is more or less linear. The result suggests that fragmentation of the chain and formation of carbonyl groups are joint processes.

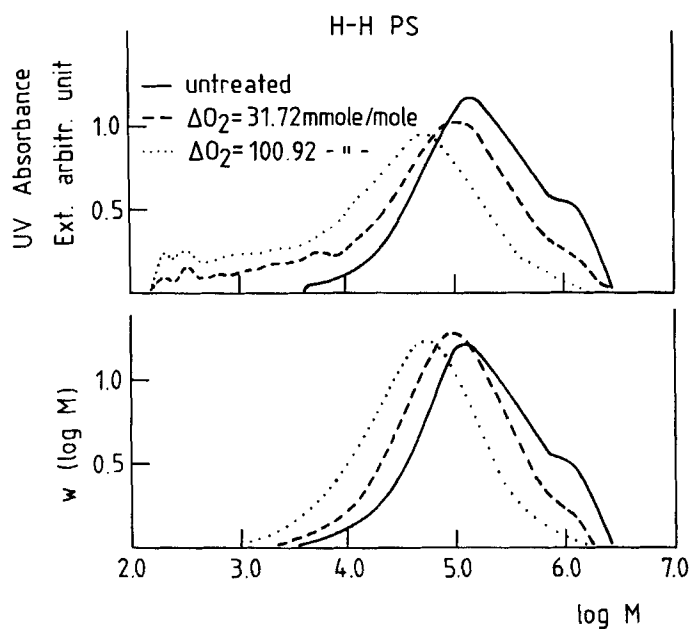


FIG. 20. Mass and UV distribution curves of untreated and photooxidized H-HPS.

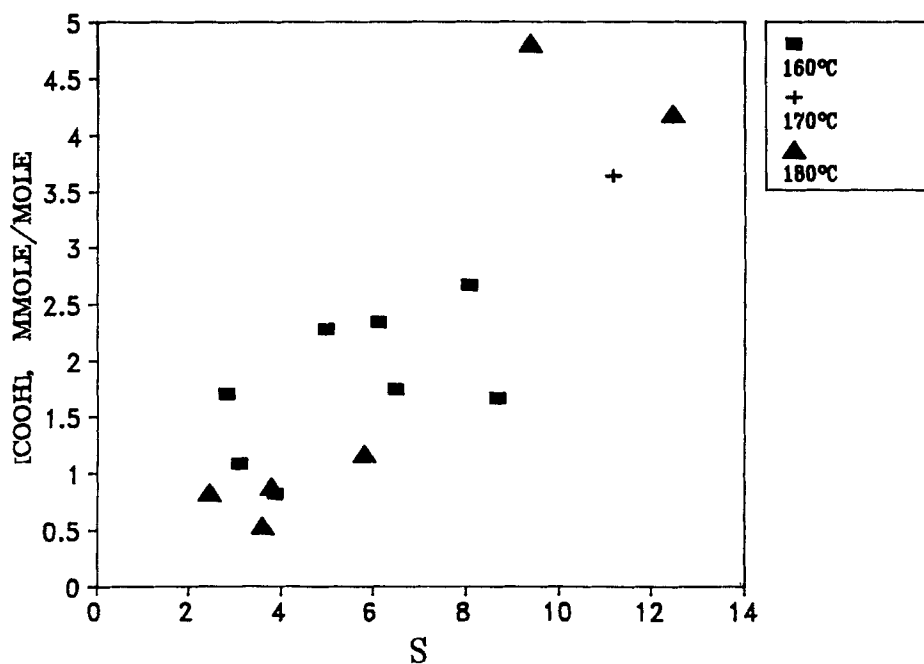


FIG. 21. Correlation between the number of carboxyl groups and the average number of scissions in the thermal oxidation of H-HPS.

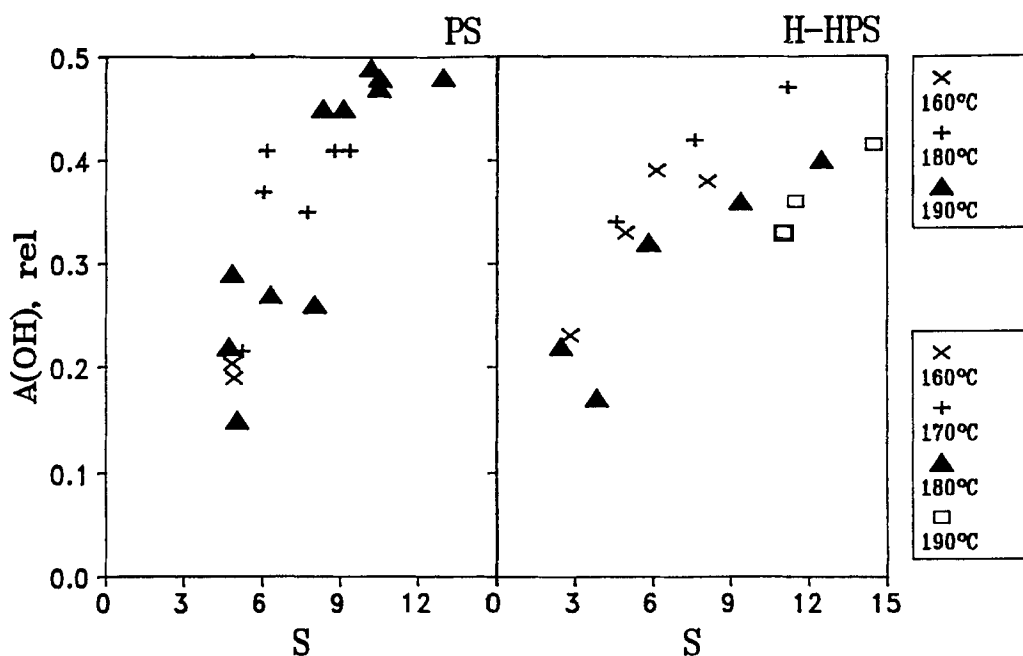


FIG. 22. Correlation between the integral IR absorption of $-OH$ groups and the average number of scissions in the thermal oxidation of head-to-tail PS and H-HPS.

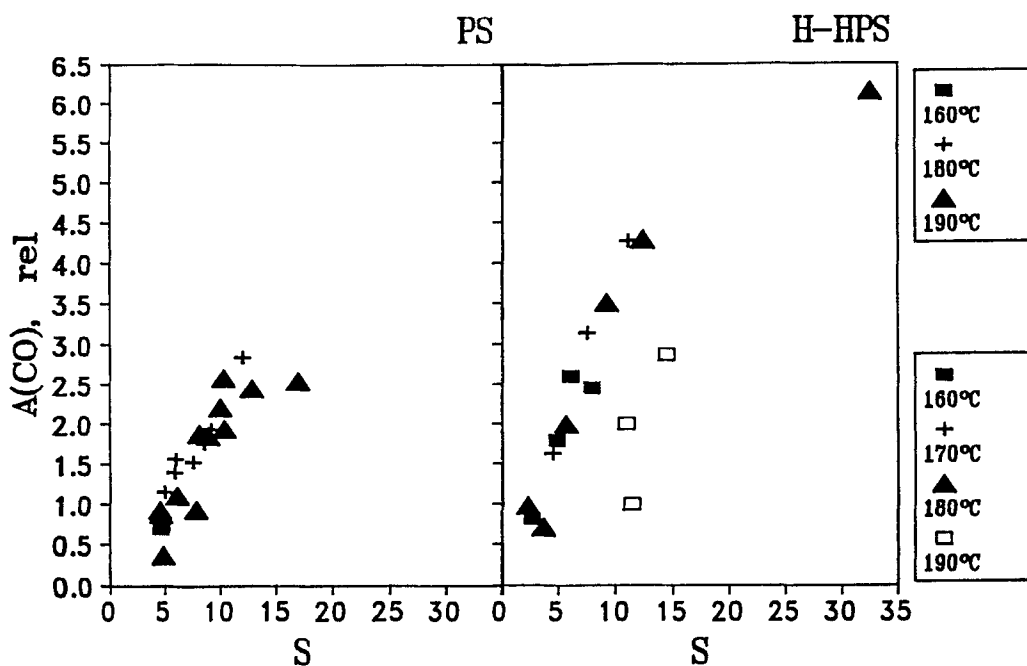


FIG. 23. Correlation between the integral IR absorption of $>CO$ groups and the average number of scissions in the thermal oxidation of head-to-tail PS and H-HPS.

In the photooxidation of head-to-tail PS, as indicated in Fig. 16, a very slight fragmentation was observed. That is, no relationships could be detected similar to those found in thermooxidation between the functional groups and s values.

REFERENCES

- [1] (a) *Encyclopedia of Polymer Science and Engineering*, Vol. 16, Wiley, New York, 1989, pp. 180–193. (b) *Degradation and Stabilization of Polymers*, Vol. 1, H. H. G. Jellinek (ed.), Elsevier, Amsterdam, 1983, Chaps. 1 and 2.
- [2] G. Mood, D. H. Solomon, and R. I. Willing, *Macromolecules*, **21**, 857 (1988).
- [3] N. A. Weir, P. Kutok, and K. Whiting, *Polym. Degrad. Stab.*, **24**, 247 (1989).
- [4] G. Moad, D. H. Solomon, and R. I. Willing, *Macromolecules*, **21**, 855 (1988).
- [5] W. Klopffer, *Eur. Polym. J.*, **11**, 203 (1975).
- [6] G. Geuskens, P. Bastin, Q. Lu Winh, and M. Rens, *Polym. Degrad. Stab.*, **3**, 295 (1980–81).
- [7] N. Grassie and N. A. Weir, *J. Appl. Polym. Sci.*, **9**, 987 (1965).
- [8] B. Rånby and J. F. Rabek, *Appl. Polym. Symp.*, **35**, 243 (1979).
- [9] G. Geuskens, in *Developments in Polymer Degradation* Vol. 3 (N. Grassie, ed.), Applied Science Publishers, London, 1981, Chap. 7, p. 207.
- [10] H. C. Beachell and L. H. Smiley, *J. Polym. Sci., Part A-1*, **5**, 1635 (1967).
- [11] L. Dulog and K. H. David, *Makromol. Chem.*, **145**, 67 (1971).
- [12] H. H. G. Jellinek and S. N. Lipovac, *Macromolecules*, **3**, 231 (1970).
- [13] V. M. Goldberg, V. N. Esenin, and G. E. Zaikov, *Vysokomol. Soedin.*, **A28**, 1634 (1986).
- [14] M. Iring, E. Földes, M. Szesztay, and F. Tüdös, *J. Macromol. Sci. – Chem.*, **A27**, 1657 (1990).
- [15] J. Lucki, J. F. Rabek, and B. Rånby, *Appl. Polym. Symp.*, **35**, 275 (1979).
- [16] B. Dickens and J. Marchal, *Polym. Degrad. Stab.*, **6**, 211 (1984).
- [17] L. S. Corley, H. Inoue, M. Helbig, O. Vogl, K. Seki, and D. Tirrell, *Macromol. Synth.*, **9**, 31 (1985).
- [18] M. Kryszewski, J. Jachowicz, and O. Vogl, *MMI Press Symp.*, **2**, 273–282 (1982).
- [19] M. Iring, T. Kelen, and F. Tüdös, *Eur. Polym. J.*, **11**, 631 (1975).
- [20] Zs. László-Hedvig, M. Iring, G. Bálint, T. Kelen, and F. Tüdös, *Appl. Polym. Symp.*, **35**, 161 (1979).
- [21] Zs. László-Hedvig, M. Szesztay, I. Pupek, and F. Tüdös, *Angew. Makromol. Chem.*, **122**, 51 (1984).
- [22] F. Tüdös, Zs. Fodor, and M. Iring, in *Oxidation Inhibition in Organic Materials*, Vol. II (J. Pospisil and P. P. Klemchuk, eds.), CRC Press, Boca Raton, Florida, Chap. 5.
- [23] M. Iring, T. Kelen, Zs. Fodor, and F. Tüdös, *Polym. Bull.*, **7**, 489 (1982).

Received January 6, 1992

Revision received March 9, 1992